Neurobiology of Disease 229 (2026) 107608

Contents lists available at ScienceDirect

Neurobiology of Disease

journal homepage: www.elsevier.com/locate/ynbdi

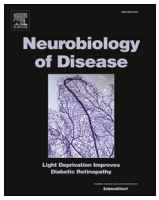

Motor coordination and behavioural deficits in a mouse model of KMT2B-related dystonia

Philip Harrer [a,b,*], Andrea Kranz [c], Lore Becker [d], Lillian Garrett [d], Sabine M. Hölter [d], Adrián Sanz-Moreno [d], Oana V. Amarie [d], Birgit Rathkolb [d,e,f], Stefanie Leuchtenberger [d], Valerie Gailus-Durner [d], Helmut Fuchs [d], Martin Hrabě de Angelis [d,e,g], Alice Saparov [a,b], Celestine Sieber [a,b], Volker Kittke [a,b], Nazanin Mirza-Schreiber [a,b,h], A. Francis Stewart [c,i], Juliane Winkelmann [a,b,j,k], Konrad Oexle [a,b,h], Amanda Pocratsky [l], Michael Zech [a,b,m]

[a] *Institute of Human Genetics, School of Medicine and Health, Technical University of Munich, Munich, Germany*
[b] *Institute of Neurogenomics, Helmholtz Zentrum München, Munich, Germany*
[c] *Genomics, Center for Molecular and Cellular Bioengineering, Biotechnology Center, Technische Universität Dresden, Dresden, Germany*
[d] *Institute of Experimental Genetics, German Mouse Clinic, Helmholtz Zentrum München, German Research Center for Environmental Health GmbH, Neuherberg, Germany*
[e] *German Center for Diabetes Research (DZD), Neuherberg, Germany*
[f] *Institute of Molecular Animal Breeding and Biotechnology, Gene Center, Ludwig-Maximilians-University München, Munich, Germany*
[g] *Chair of Experimental Genetics, TUM School of Life Sciences, Technische Universität München, Freising, Germany*
[h] *Neurogenetic Systems Analysis Group, Institute of Neurogenomics, Helmholtz Zentrum München, German Research Center for Environmental Health, Munich, Germany*
[i] *Key State Laboratory of Microbial Research, Shandong University, Qingdao, Shandong, China*
[j] *DZPG, Deutsches Zentrum Für Psychische Gesundheit, Munich, Germany*
[k] *Munich Cluster for Systems Neurology, SyNergy, Munich, Germany*
[l] *Department of Neuromuscular Diseases and UCL Queen Square Motor Neuron Disease Centre, UCL Queen Square Institute of Neurology, University College London, London, UK*
[m] *Institute for Advanced Study, Technical University of Munich, Garching, Germany*

ARTICLE INFO

Keywords:
KMT2B
Histone methyltransferase
Dystonia
Mouse model
Motor coordination
Sensorimotor gating
Dystonic-like paw posturing

ABSTRACT

Introduction: Pathogenic variants in *KMT2B* cause early-onset dystonia, but a mouse model that has undergone comprehensive, dystonia-oriented phenotyping is lacking.
Methods: We conducted detailed phenotyping on heterozygous *Kmt2b* constitutive knockout mice and wild-type littermates, assessing growth, neurobehavioural traits, motor coordination, sensorimotor gating, social behaviour and metabolic parameters, combined with striatal RNA sequencing.
Results: *Kmt2b* knockout mice of both sexes were viable but significantly smaller and lighter than littermate controls. Knockouts were hyperlocomotive in the open field and showed approximately two-fold larger acoustic startle responses; unexpectedly, prepulse inhibition was enhanced rather than reduced at all prepulse intensities. On the balance beam, knockouts crossed more slowly and paused more frequently; female knockouts also paused more on the ladder rung task. Frame-by-frame video analysis revealed a claw-like hindpaw posture characterized by abnormal inward flexion of the digits. Knockout mice spent less time investigating a novel conspecific, while social recognition memory remained intact. Striatal RNA sequencing confirmed reduction of *Kmt2b* transcript to approximately half of control levels and identified 177 differentially expressed genes, including *Maob*, encoding monoamine oxidase B; gene set enrichment analysis implicated neurodevelopmental, glial and mitochondrial processes. Nociception, vision, body-weight-adjusted grip strength, and clinical chemistry and haematological measures were largely unaffected.
Conclusion: Heterozygous *Kmt2b* knockout mice show hyperlocomotion, altered sensorimotor gating, impaired motor coordination with dystonic-like paw posturing and reduced sociability, alongside a striatal transcriptomic signature implicating neurodevelopmental processes. The model mirrors aspects of human KMT2B-related

* Corresponding author at: Institute of Neurogenomics, Helmholtz Munich, Ingolstädter Landstraße 1, 85764 Neuherberg, Germany.
E-mail address: philip.harrer@helmholtz-munich.de (P. Harrer).

https://doi.org/10.1016/j.nbd.2026.107608
Received 9 June 2026; Received in revised form 10 September 2026; Accepted 11 September 2026
Available online 11 September 2026

dystonia and provides a platform for mechanistic study; environmental or pharmacological challenge may be needed to unmask overt dystonic features.

1. Introduction

Dystonia is a heterogeneous movement disorder characterized by sustained and/or intermittent muscle contractions that result in abnormal movements and postures. Among the genetic causes of childhood-onset generalized dystonia, heterozygous variants in *KMT2B* encoding the lysine-specific histone methyltransferase 2B have emerged as a prominent contributor (Zech et al., 2016; Meyer et al., 2017). First described in 2016, subsequent studies have identified over 100 distinct mutations in *KMT2B* in patients with early-onset dystonia (Zech et al., 2016; Meyer et al., 2017; Ciolfi et al., 2021; Zech et al., 2019). Most *KMT2B* mutations are heterozygous de novo loss-of-function changes, in keeping with haploinsufficiency of *KMT2B* (Zech et al., 2016; Meyer et al., 2017; Ciolfi et al., 2021; Zech et al., 2019). A smaller fraction of pathogenic variants are missense mutations affecting conserved domains in line with a loss-of-function mechanism suggested by their location within these domains (Zech et al., 2017). Together, these findings establish *KMT2B* mutations as frequent causes of monogenic childhood dystonia (Carecchio et al., 2019).

Clinically, KMT2B-associated dystonia typically begins in childhood with focal onset and progresses in a caudo-rostral manner to generalized dystonia with cranio-cervical involvement (Zech et al., 2019; Carecchio et al., 2019). Many patients present with a complex neurodevelopmental syndrome: in addition to dystonic movements, affected individuals often exhibit intellectual disability, developmental delay, and/or psychiatric comorbidities (Carecchio et al., 2019; Cif et al., 2020; Faundes et al., 2018). Notably, considerable phenotypic variability and incomplete penetrance have been reported even among carriers of the same *KMT2B* variant (Carecchio et al., 2019; Stehr et al., 2025).

As a member of the COMPASS-like/Trithorax family of H3K4 methyltransferases, KMT2B is one of six related enzymes that regulate H3K4 methylation in mammals (Glaser et al., 2006). Unlike its paralogs, KMT2B acts preferentially at bivalent promoters - genomic loci co-marked by activating H3K4me3 and repressive H3K27me3 - where it maintains the chromatin state of developmentally regulated genes, co-occupying these loci with Polycomb repressive complexes in specific cellular contexts (Glaser et al., 2009; Denissov et al., 2014). Consistent with this non-redundant developmental role, homozygous loss of *Kmt2b* causes embryonic lethality before E11.5 in mice (Glaser et al., 2006). Beyond its role in embryogenesis, KMT2B is required for neuronal gene regulation in the adult brain: conditional knockout of *Kmt2b* in excitatory forebrain neurons impairs hippocampus-dependent memory consolidation, accompanied by reduced H3K4me2/3 and down-regulation of a specific set of neuronal plasticity genes (Kerimoglu et al., 2013). Comparative analyses further demonstrate that KMT2B and its paralog KMT2A regulate largely non-overlapping genomic regions and distinct molecular pathways in hippocampal neurons, underscoring the functional specificity of individual H3K4 methyltransferases in the mature nervous system (Kerimoglu et al., 2017). Together, these findings establish KMT2B as a context-specific chromatin regulator with non-redundant roles in both embryonic development and adult neuronal gene regulation.

Despite these advances – including improvements in molecular diagnostics such as a specific blood DNA methylation episignature for KMT2B-associated dystonia (Mirza-Schreiber et al., 2022) - the pathophysiological link between KMT2B deficiency, dysfunction of the broader motor control network, and the full spectrum of associated comorbidities remains incompletely understood. Compared to other genetic forms of dystonia, *KMT2B*-associated dystonia has been less explored in animal models. Studies on other dystonia-causing genes in vivo have shown that rodent models may fail to recapitulate overt dystonic-like movements but can reveal subtle neurological deficits and pathogenic mechanisms (Berryman et al., 2023). The absence of a comprehensively characterized heterozygous *Kmt2b* knockout model represents a specific gap that limits progress in understanding this form of dystonia.

We present a detailed phenotypic characterization of mice carrying a heterozygous *Kmt2b* constitutive knockout allele, revealing a spectrum of neurobehavioural abnormalities that recapitulate aspects of human KMT2B-related dystonia. Because KMT2B is a broadly expressed chromatin regulator with pleiotropic developmental functions, and because KMT2B-related disease extends beyond isolated dystonia to non-motor features such as autism, attention deficit hyperactivity disorder, intellectual impairment, and short stature, we hypothesized a priori that heterozygous Kmt2b loss would disrupt multiple, partially independent neurodevelopmental circuits rather than produce an isolated motor sign. Assays were therefore selected to probe evidence across different circuit-relevant domains predicted to be vulnerable to *Kmt2b* haploinsufficiency: skilled motor coordination and fine motor control, assessed with balance beam, ladder rung walking, and grip strength, modelling the core motor domain of KMT2B-related dystonia; basal ganglia and sensorimotor gating circuitry, assessed with open field locomotor activity and acoustic startle and PPI, given the recognized involvement of basal ganglia circuits in dystonia; social and communicative behaviour, assessed with social discrimination and vocalisation during handling, reflecting the neurodevelopmental and psychiatric comorbidities reported in *KMT2B*-mutated patients; and general neurological, sensory and metabolic status, assessed with modified SHIRPA, nociception, vision and growth, together with hearing inferred from preserved acoustic startle responses and olfactory function inferred from investigation behaviour in the social discrimination test, to exclude generalized impairment as an alternative explanation for the circuit-specific findings. This framework guided both assay selection and interpretation. The present model provides a well-characterized experimental platform for future mechanistic investigations into the pathogenesis of KMT2B-related dystonia.

2. Methods

2.1. Generation of the Kmt2b knockout mouse model and housing conditions

Kmt2b heterozygous knockout mice were generated from the *Kmt2b*^{tm1Afst} (MGI:3623309) targeted allele created in E14 embryonic stem (ES) cells by inserting a multipurpose cassette (Glaser et al., 2006). The targeting cassette carried a 3′ loxP site, and a second loxP replaced the endogenous *Apa*LI site in intron 2. Two correctly targeted E14 ES-cell clones were used to generate chimeras, which were subsequently bred to C57BL/6 to establish the line. RT-PCR confirmed truncation of the transcript upstream of exon 2, establishing a null allele (Glaser et al., 2006). Germline chimeras were obtained, and heterozygous offspring were viable and used for experiments, whereas homozygous mutants were embryonic lethal before ~E11.5 as reported (Glaser et al., 2006). The line was backcrossed onto a C57BL/6JolaHsd background for at least four generations before phenotypic analysis. Experimental mice were obtained by intercrossing *Kmt2b* heterozygotes; wild-type littermates were used as controls.

All animal procedures were approved by the responsible authority of the district government of Upper Bavaria and conducted in accordance with the European Directive 2010/63/EU. All mice were housed in individually ventilated caging (IVC) systems (Sealsafe Plus, GM 500, Tecniplast, Buguggiate, Italy) under specific pathogen-free conditions

(GMC), with a maximum of five adult mice per cage. The IVC systems operated under positive pressure. Mice received autoclaved wood chips (Lignocel Select Fine, J. Rettenmaier & Soehne GmbH, Rosenberg, Germany) and paper strips (Arbocel Crinclets Natural, Rettenmaier & Soehne GmbH) as bedding and nesting material, irradiated standard rodent diet (Altromin 1314, Altromin Spezialfutter GmbH, Lage, Germany), and sterile-filtered tap water ad libitum.

Cages were changed weekly in laminar flow changing stations. The light cycle was maintained at 12 h/12 h light/dark with a 10-min dimming period to simulate sunrise and sunset. Environmental parameters were controlled at 22 ± 2 °C and 55 ± 10% relative humidity. Facility access was restricted via electronic key control and airlocks, with mandatory use of personal protective equipment (autoclaved trousers and shirts, dedicated shoes, surgical masks, hair bonnets, and gloves). Health monitoring followed FELASA guidelines and was performed quarterly by exhaust air dust PCR analysis for all listed agents through a commercial diagnostic laboratory.

2.2. Genotyping

Genotyping was performed by PCR on genomic DNA using primers flanking the modified locus (forward: 5′-GTCCTGTGTTCAGTCCAAGGTAG-3′; reverse: 5′-GGAGAACAGTTGTGGGGAGATGGGTC-3′), yielding a ~ 130 bp product for the wild-type allele and a ~ 230 bp product for the targeted allele. Cycling (hot-start) conditions were: 95 °C for 5 min; 35 cycles of 95 °C for 30 s, 58 °C for 30 s, and 68 °C for 1 min; followed by 68 °C for 7 min.

2.3. Phenotyping

The phenotyping cohort was subjected to a comprehensive neurobehavioural screening pipeline at the German Mouse Clinic (GMC) starting at 9 weeks of age when mice have reached early adulthood (Fuchs et al., 2011; Fuchs et al., 2018). Phenotyping was performed on $N = 15$ littermate controls and $N = 15$ *Kmt2b* heterozygous knockout mice of both sexes ($N = 60$ total). Tests were chosen for covering major behavioural (e.g. exploratory drive and anxiety-related behaviour measured in the Open Field Test, and social interest and social recognition memory measured in the Social Discrimination Test), motor (e.g. locomotor activity, motor coordination from assessing general movement in SHIRPA over more skilled movement with rotarod, balance beam and final ladder for including also more fine-tuned movements) and sensory domains (olfaction, sensorimotor gating, hearing, vision, nociception). Animals were given sufficient recovery time between tests leading to a testing range of 9 to 39 weeks.

To minimise experimental bias, the daily testing order was randomised within sex and genotypes were balanced across sessions. The experimenter was blind to genotype in all assays in which the experimenter administers, scores, or otherwise directly influences the measurement: modified SHIRPA, dysmorphology screening, grip strength, rotarod, balance beam, ladder rung walking, and the hot plate test. Balance beam sessions were additionally video-recorded, and hindpaw posture was scored frame-by-frame offline by a second observer blind to genotype. The social discrimination test was not conducted blind, but investigation times were scored offline by an observer blind to genotype. Open field, acoustic startle and prepulse inhibition, optomotor assessment of visual acuity (OptoDrum, Striatech GmbH), and clinical chemistry and haematology were not conducted blind, as the outcome measure is generated by the apparatus or analyser without experimenter scoring. Automated acquisition removes observer bias from the measurement itself but does not exclude genotype-related differences in handling prior to testing. All animals were therefore handled by the same experimenter following a standardised procedure. Data capture and QC were handled via the GMC's ISO-certified workflows and standardised SOPs with full metadata logging (date/time, experimenter, equipment ID).

2.4. Developmental and neurological assessments

Growth and Dysmorphology: Mice were monitored from birth for general health and developmental milestones. Body weight was measured at regular intervals prior to each test and body length was recorded at the end of the pipeline (39 weeks). Gross morphology and any dysmorphic features were assessed by systematic observation. At ~10 weeks, mice underwent a modified SHIRPA neurological screen (Rogers et al., 1997) to assess motor behaviours that are consistent with changes in muscle tone, motor neuron function, cerebellar function, sensory responses, and/or autonomic signs. This screen included observation of undisturbed behaviour in a novel arena, reflex testing (including contact righting), and notation of any abnormal behaviours or physical anomalies.

Open field: The 20-min Open Field (OF) test was carried out using the ActiMot system (TSE, Germany) as described previously (Garrett et al., 2012; Hölter et al., 2015a). The arena was made of transparent and infra-red light-permeable acrylic with a smooth floor (internal measurements: 45.5 × 45.5 × 39.5 cm, 200 lx in middle). The testing took place at the beginning of the light phase, but no earlier than 1 h after lights on.

Grip Strength: Forelimb and hindlimb grip strength was measured at 10 weeks of age ($N = 15$ female and $N = 14$ male littermate control, $N = 15$ female and $N = 15$ male *Kmt2b* knockout mice; $N = 59$ total) using a grip strength meter (Bioseb). Each mouse was allowed to grasp a metal grid with either its forepaws or all four paws and then was gently pulled back at the base of the tail until paw grip was released. Three trials were recorded for each configuration. The mean grip force from the three trials was calculated for each animal. For inclusion in the analysis, animals were required to complete a minimum of two out of the three trials.

Motor Coordination and Balance: Coordination and balance were evaluated with three assays: an accelerating rotarod, balance beams of varying diameters (28 mm, 18 mm, 12 mm, and 6 mm, wooden cylinder beams) at 29 weeks of age, and a horizontal ladder task at 30 weeks of age. For the rotarod test (Bioseb) at 11 weeks of age, $N = 58$ mice ($N = 15$ female and $N = 14$ male littermate control, $N = 14$ female and $N = 15$ male *Kmt2b* knockout mice) were placed on a rotating cylinder accelerating from 4 to 40 rpm over 300 s; the latency to fall off (or to complete one passive full rotation hanging on) was recorded. Each mouse performed three trials (15 min inter-trial intervals), and the mean latency to fall was analysed. For the beam walking assay, $N = 58$ mice ($N = 15$ female and $N = 14$ male littermate control, $N = 14$ female and $N = 15$ male *Kmt2b* knockout mice) were trained to traverse a narrow, elevated beam (various diameters, 50 cm above a padded surface). Time to cross, number of stops (>1 s pauses; exclusion of stops due to distracted behaviours, e.g. sniffing), and number of foot slips (a true slip was defined as an event in which a paw lost full contact and fell entirely off the beam surface, beyond just the toes) were recorded as performance metrics. If a mouse hesitated, gentle prodding was applied to the hindquarters to encourage movement, and ample rest was provided between trials. In the ladder rung task, $N = 57$ mice ($N = 15$ female and $N = 14$ male littermate control, $N = 13$ female and $N = 15$ male *Kmt2b* knockout mice) crossed a 1 m horizontal ladder with irregularly spaced rungs (after one training trial). Each mouse performed three test runs. Performance was quantified by the total crossing time, the number of stops, and the number of forelimb or hindlimb slip errors, defined as instances in which a paw was placed on a rung but subsequently lost grip, slipped off, descended below rung level, and required correction. The ladder was cleaned between trials. Videotaping was performed using a handheld Canon SX620HS. Balance beam recordings were additionally analysed frame by frame for hindpaw posture in a subset of animals ($N = 3$ male *Kmt2b* knockout mice and $N = 3$ male littermate controls; selected at random). The presence or absence of the claw-like posture was scored for each animal and compared between genotypes.

Acoustic Startle and Prepulse Inhibition: Supraspinal

sensorimotor gating was assessed using acoustic startle reflex and prepulse inhibition (PPI) paradigms. Startle responses were measured in sound-attenuating chambers (Med Associates) with a 65 dB background white noise. After 5 min of acclimation, startle trials (40 ms noise bursts at 110 dB) were presented. In PPI trials, the 110 dB startle pulse was preceded by a 50 ms prepulse (at 67, 69, 73, or 81 dB). A series of startle-only and prepulse + startle trials were presented in pseudorandom order with 20–30 s inter-trial intervals. Startle amplitude was recorded on each trial, and % PPI was calculated as the reduction in startle response magnitude on prepulse trials relative to startle-alone trials. Startle amplitude was defined as the peak whole-body startle response detected by the platform-mounted transducer.

The startle apparatus was calibrated before testing, and control and knockout animals were tested concurrently in the same sessions; startle amplitudes recorded from control animals in response to the 110 dB pulse were within the expected range for this strain in our setup, making transducer or amplifier saturation an unlikely explanation for the genotype difference. Startle amplitudes were not normalised to body weight. Because platform-mounted transducers register larger deflections in heavier animals, any body-weight-related bias would act against the observed effect of knockout mice being significantly lighter than controls yet showing larger startle amplitudes.

Social Discrimination Test: Social interest and recognition memory were evaluated using a two-trial social discrimination paradigm as described previously (Hölter et al., 2015b). Subject mice were isolated 2 h prior to testing to increase social motivation. In a 4 min sample trial, a stimulus mouse (ovariectomised (OVX) female to minimise hormonal variability) was introduced to the cage with the subject mouse and both were allowed to interact freely. After a 2 h inter-trial interval, the subject mouse was reexposed for a second 4 min test trial with the now-familiar OVX mouse from the first trial and a novel OVX mouse. The olfactory investigation time of the subject mouse with stimulus mice during each trial were recorded. A social recognition index was calculated as the proportion of total investigation time spent investigating the novel animal. The arena was cleaned between trials to eliminate residual olfactory cues.

2.5. Sensory and physiological assessments

Visual Acuity: Visual acuity was tested using an optomotor reflex assay (OptoDrum, Striatech GmbH) (Prusky et al., 2004). Mice were placed on a platform surrounded by computer monitors displaying rotating high-contrast vertical sine-wave gratings (12 deg./s). Reflexive head movements (optomotor responses) were monitored to determine the threshold spatial frequency the animals could reliably track, to identify their visual acuity.

Thermal Nociception: Acute pain sensitivity was assessed with a hot-plate test. Mice were placed on a 52 °C hot plate (TSE Systems) enclosed by a 20 cm-high Plexiglas cylinder. The latency to exhibit a nociceptive response (e.g. hind paw lick, shake/flutter, or jump) was recorded, with a cutoff time of 30 s to prevent tissue injury. Each mouse was tested only once to avoid sensitization from repeated exposure.

2.6. Clinical chemistry and haematology

At 39 weeks of age, remaining mice ($N = 57$; $N = 14$ male and $N = 15$ female littermate controls and $N = 15$ male and $N = 13$ female heterozygous *Kmt2b* knockout mice) were anaesthetised with isoflurane (5% in compressed air), and blood was collected via retro-orbital puncture. Animals were immediately killed under anaesthesia by cranio-cervical dislocation; a subset was killed by CO_2-inhalation to allow specific tissue collection. For plasma analyses, blood was collected in Li-heparin-coated tubes (Kabe-Labortechnik GmbH, Germany) and centrifuged within 2 h of collection at 5000 ×g for 10 min at 8 °C. Plasma was distributed into aliquots and analysed using an automated clinical chemistry analyser (AU480, Beckman Coulter, Germany) for a panel of parameters including metabolic markers, liver and renal function, lipid profile, electrolytes, and iron metabolism. Plasma for clinical chemistry was transferred into 1.5 ml tubes (Eppendorf, Germany), vortexed, and centrifuged again (5000 ×*g*, 10 min, 8 °C) before analysis. For haematology analyses, 50 µl blood was collected in EDTA-coated end-to-end capillaries (Kabe-Labortechnik GmbH, Germany) and diluted 1:7 with Sysmex Cellpack DCL buffer (Sysmex Deutschland GmbH, Germany). Diluted samples were analysed within 2 h of collection using an automated haematology analyser (Sysmex XN1000V, mouse settings, pre-dilution mode) to obtain complete blood counts including red and white blood cell counts.

2.7. RNA sequencing and transcriptomic analysis

Striatal tissue was collected from $N = 6$ heterozygous *Kmt2b* knockout mice and $N = 6$ littermate controls at 39 weeks of age. Brains were removed immediately after sacrifice, the striatum was dissected, and tissue was snap-frozen in liquid nitrogen and stored at −80 °C until processing. Total RNA was extracted using the RNeasy mini kit (Qiagen, Netherlands) according to the manufacturer's instructions. RNA quantity and integrity were assessed using the Bioanalyzer 2100 (Agilent Technologies, USA), with all samples showing RIN values >9. Sequencing libraries were prepared from 1000 ng of total RNA using TruSeq Stranded mRNA library preparation kit (Illumina, USA) with poly-A selection, and sequenced on a HiSeq4000 in paired-end 150 bp mode to a minimum of 30 million mapped clusters (60 million mapped reads) per sample. Sequencing data have been deposited in the NCBI Gene Expression Omnibus (GEO: GSE346547).

Reads had been aligned previously to mm9 (NCBIM37) with STAR v2.4.2a (Dobin et al., 2013); counts were re-analysed with DESeq2 v1.34.0 (Love et al., 2014) in R (R Core Team, 2015). Genes with fewer than 10 total counts across all samples were excluded prior to model fitting, following the package's standard pre-filtering recommendation. Significance was assessed by the Wald test with Benjamini–Hochberg correction for multiple testing, and genes with an adjusted p-value <0.05 were considered differentially expressed. No log fold-change shrinkage was applied, and fold changes are reported as maximum-likelihood estimates.

Gene set enrichment analysis was performed with clusterProfiler v4.14.6 (Wu et al., 2021) against Gene Ontology Biological Process terms, using the org.Mm.eg.db annotation database. All genes retained after count filtering were ranked by their DESeq2 Wald test statistic, so that the analysis assesses the distribution of each gene set across the complete ranked transcriptome rather than being restricted to individually significant genes. Gene sets reaching a Benjamini-Hochberg adjusted p-value<0.05 were considered significantly enriched, and the 20 most significantly enriched terms were visualized.

2.8. Statistical analysis

All data were analysed using GraphPad Prism 9 and R 4.6.1 (R Core Team, 2015). Two-way ANOVA with Tukey post-hoc was used as the default approach; parameters for which body weight was a meaningful covariate were analysed by ANCOVA with body weight as covariate, parameters with a strong sex effect were analysed separately by sex with unpaired t-tests, and non-parametric tests were substituted where normality was violated. The assumption was violated for the number of stops on the balance beam and on the horizontal ladder, which were therefore analysed by Wilcoxon rank-sum (Mann–Whitney U) tests separately by sex, and for the balance beam at each beam width. Non-parametric parameters are summarised as median and interquartile range and displayed as box-and-whisker plots; all parameters analysed with parametric tests are summarised and displayed as mean ± SD. Categorical parameters were analysed using two-sided Fisher's exact tests, except for the frame-by-frame hindpaw posture analysis. For this parameter a one-sided Fisher‘s test was specified beforehand, based on

the directional hypothesis that dystonic-like posturing would occur in knockout animals and not in wild-type controls; the opposite direction would not be interpretable.

A p-value <0.05 was used as the threshold for statistical significance. Given the exploratory, hypothesis-generating nature of this phenotyping pipeline no correction for multiple testing was applied, consistent with established practice in systematic mouse phenotyping studies (Fuchs et al., 2011; Fuchs et al., 2018); statistically significant findings should therefore be interpreted as indicative rather than confirmatory. When evaluating biological relevance, the magnitude of group differences was considered alongside p-values.

Transcriptomic data were analysed separately as described above. In contrast to the phenotyping parameters, RNA sequencing and gene set enrichment results were corrected for multiple testing using the Benjamini-Hochberg procedure.

3. Results

3.1. Growth reduction in Kmt2b knockout mice

Heterozygous *Kmt2b* knockout mice showed no gross developmental abnormalities in the pre-weaning period. Both male and female *Kmt2b* knockout mice gained weight throughout post-weaning maturation but had significantly lower body weights on average at almost every time point assessed (Fig. 1A). Furthermore, *Kmt2b* knockout mice of both sexes exhibited decreased body length compared to controls at 39 weeks of age ($p < 0.01$; Fig. 1A). Despite their smaller size, *Kmt2b* knockouts showed normal general health, appearance, and vitality.

3.2. Behavioural abnormalities in open field, prepulse inhibition and social discrimination testing

In the open field test, 9-week-old *Kmt2b* heterozygous knockout mice ($N = 14$ females and $N = 15$ males) showed signs of hyperlocomotion compared to littermate controls of both sexes ($N = 15$ per sex). Increased locomotor activity of knockout mice of both sexes was evident within the first 5 min of novel environment exposure with increased distance travelled relative to controls, and this persisted across the whole 20-min observation time leading to a significant increase in total travel distance for *Kmt2b* knockouts (17,283.9 vs. 21,954.2 cm in females; 19,696.9 vs. 21,932.1 cm in males; 2-way ANOVA genotype effect: $p = 0.002$; Fig. 2A, left panel; Supplementary Table S1). The average locomotor speed was also significantly increased in *Kmt2b* knockout mice relative to controls (15.4 vs. 19.7 cm/s in females; 17.6 vs. 19.4 cm/s in males; 2-way ANOVA genotype effect: $p = 0.003$; Fig. 2A, right panel; Supplementary Table S1). Notably, there were no genotype-related differences in time spent in the centre of the arena, the proportion of distance travelled in the centre, or the number of rears. Although knockouts showed a significantly higher number of entries into the centre zone ($p = 0.045$; Supplementary Table S1), this is likely attributable to their overall increase in locomotor activity rather than reflecting altered anxiety-related exploration, as the proportion of time and distance in the centre did not differ between genotypes. Together, these findings indicate increased baseline locomotor activity in *Kmt2b* knockout mice without evidence for altered anxiety-related exploration in the open field.

In acoustic startle and prepulse inhibition testing, 9-week-old *Kmt2b* knockout mice ($N = 14$ females, $N = 15$ males) demonstrated altered sensorimotor processing compared to littermate controls of both sexes ($N = 15$ per sex). Knockout mice showed a significantly increased acoustic startle response to a 110 dB sound burst, with approximately two-fold higher startle amplitudes in *Kmt2b* knockouts compared to controls (2-way ANOVA genotype effect: $p = 0.002$; Fig. 2B; Supplementary Table S2). When a prepulse tone preceded the startle pulse (PPI), both groups showed reduced startle responses, indicating intact prepulse inhibition. Notably, *Kmt2b* knockouts exhibited a significantly greater degree of prepulse inhibition at all prepulse intensities tested (67, 69, 73, 81 dB; Fig. 2B; Supplementary Table S2). Averaged across all prepulse intensities, percent PPI was significantly increased in knockout mice compared to controls (48.2% vs 27.3%, $p = 0.003$). Notably, this represents an enhancement rather than a reduction in sensorimotor gating - a counterintuitive direction of effect. Together, these findings indicate enhanced acoustic startle reactivity accompanied by increased prepulse inhibition in Kmt2b knockout mice, consistent with altered sensorimotor processing.

In the social discrimination test, 18-week-old *Kmt2b* knockouts ($N = 14$ females, $N = 15$ males) displayed a reduction in social investigation compared to controls ($N = 15$ per sex). When exposed to an unfamiliar conspecific (the “stimulus mouse” during sample phase), knockout mice spent less time in olfactory investigation compared to littermate controls (2-way ANOVA genotype effect: $p = 0.015$; Fig. 2C; Supplementary Table S3). In the subsequent test phase, encountering the now-familiar stimulus mouse, both knockout and littermate control mice showed a similar reduction in investigation time, indicating intact social recognition memory. However, *Kmt2b* knockouts continued to spend overall less time interacting with strangers during the novel subject test phase compared to controls (2-way ANOVA genotype effect: $p = 0.002$; Fig. 2C; Supplementary Table S3). The recognition index - reflecting the proportion of total investigation time directed towards the novel stimulus mouse - did not differ between genotypes, consistent with both groups discriminating the novel animal from the familiar one. Thus, *Kmt2b* deficiency did not impair social memory per se, but did reduce the overall drive of *Kmt2b* knockouts to engage with social stimuli, consistent with a deficit in sociability and/or social motivation.

3.3. Neurological testing reveals deficits in motor coordination during beam and ladder crossing

Littermate controls ($N = 15$ females and $N = 14$ males) and *Kmt2b* heterozygous knockout mice ($N = 14$ females and $N = 15$ males) were phenotyped using modified SHIRPA screen, a battery of tests to rapidly assess for overt abnormal behaviours that are consistent with alterations in muscle, lower motor neuron, spinocerebellar, sensory and/or autonomic functions. Using the modified SHIRPA screen, the only significant difference between knockouts and controls was vocalisation (Supplementary Table S4). While 3 female and 3 male 10-week-old controls showed vocalisation in response to gentle manipulation, none of the knockouts did so ($p = 0.023$). Together, these findings suggest that *Kmt2b* loss-of-function does not cause neurological deficits readily detectable with broadband SHIRPA testing. The reduced vocalisation in knockouts is of low penetrance and uncertain significance; in general, possible explanations include altered pain sensitivity, anxiety responsiveness, or social communication.

Specific testing of maximal grip strength using a grip strength meter revealed significantly reduced absolute forelimb grip force in 10-week-old knockout female mice (Fig. 1B, left panel, top). The grip strength of all four limbs tested together revealed no significant differences relative to controls (Fig. 1B, left panel, bottom), suggesting that female *Kmt2b* knockout mice do not have generalized muscle strength issues. Despite their smaller body weight, male *Kmt2b* knockouts did not have significantly impaired absolute grip strength. Including body weight as a covariate into the analysis, due to the strong correlation between grip strength and bodyweight, revealed similar relative grip strength in both sexes with no significant genotype effect (Fig. 1B, middle and right panel).

During testing, 4 out of 15 tested male (27%) and 3 out of 15 tested female (20%) *Kmt2b* knockout mice refused the last trial. One additional female knockout could not complete grip strength testing due to an isolated episode of tremor-like movement; no similar events were observed in this animal or any other knockout during other testing sessions, and the significance of this isolated observation remains unclear. No overt tremors were observed in control mice. Notably, no

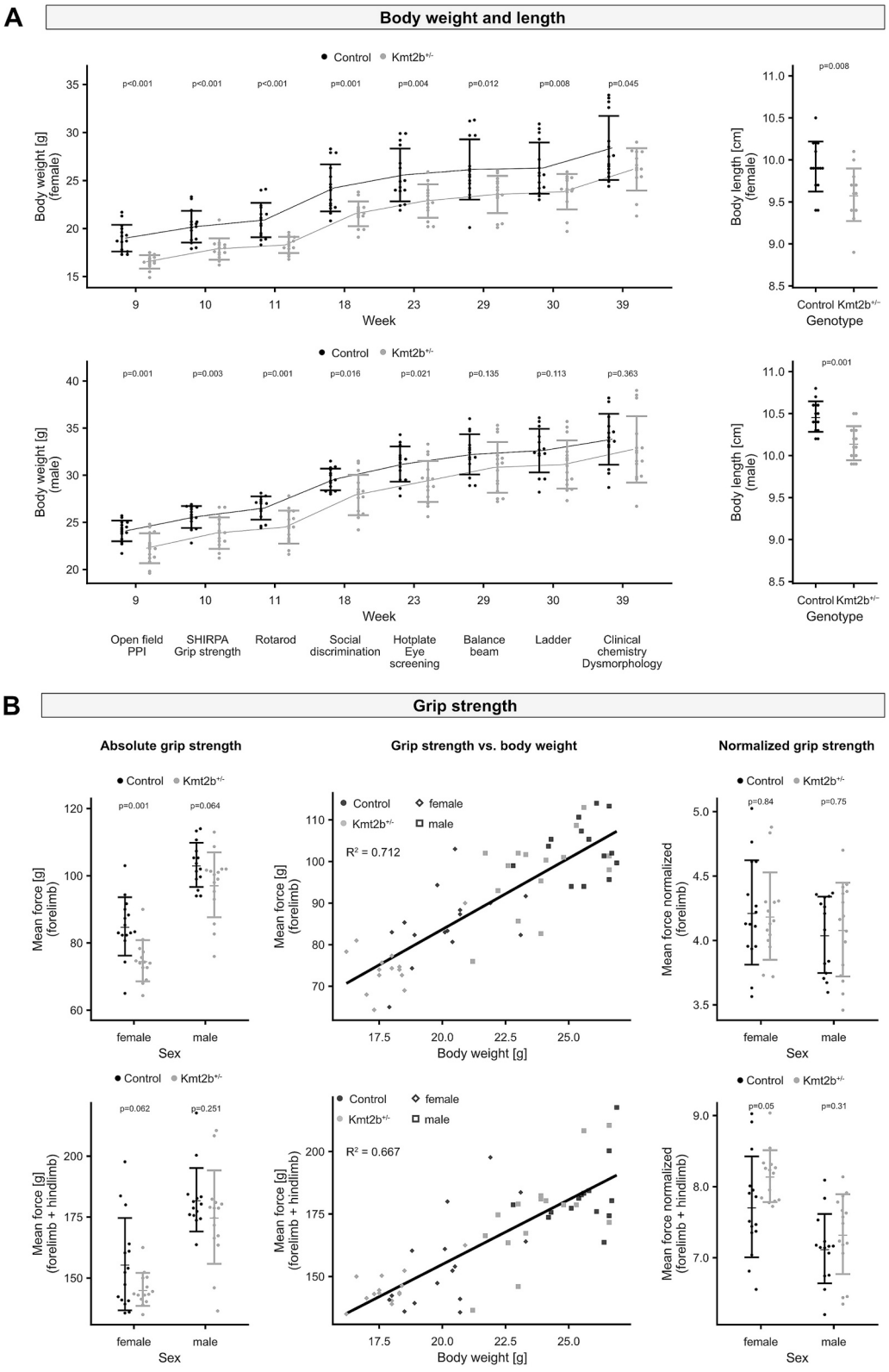

Fig. 1. Reduced growth and body-weight-dependent grip strength in *Kmt2b* heterozygous knockout mice. (A) Left: body weight of *Kmt2b* knockout and littermate control mice across the phenotyping pipeline, shown separately for females (top) and males (bottom). Knockout mice of both sexes weighed significantly less than controls at almost every time point. The experimental timeline is shown below the panel, indicating the age in weeks at which each test was performed. Right: body length at 39 weeks of age, reduced in knockout mice of both sexes. (B) Grip strength at 10 weeks of age ($N = 29$ *Kmt2b* knockouts, $N = 29$ littermate controls). The upper row shows forelimb (two-paw) measurements and the lower row combined four-limb (forelimb + hindlimb) measurements. Left: absolute mean force, showing reduced absolute forelimb force in female knockouts. Middle: mean force plotted against body weight for both genotypes and sexes, with fitted linear regression and coefficient of determination, illustrating the strong dependence of grip force on body weight. Right: mean force normalised to body weight, showing no genotype effect once body weight is accounted for. Data are shown as individual animal values with mean ± SD. *p*-values are from two-way ANOVA with Tukey post-hoc comparisons and are given above each comparison.

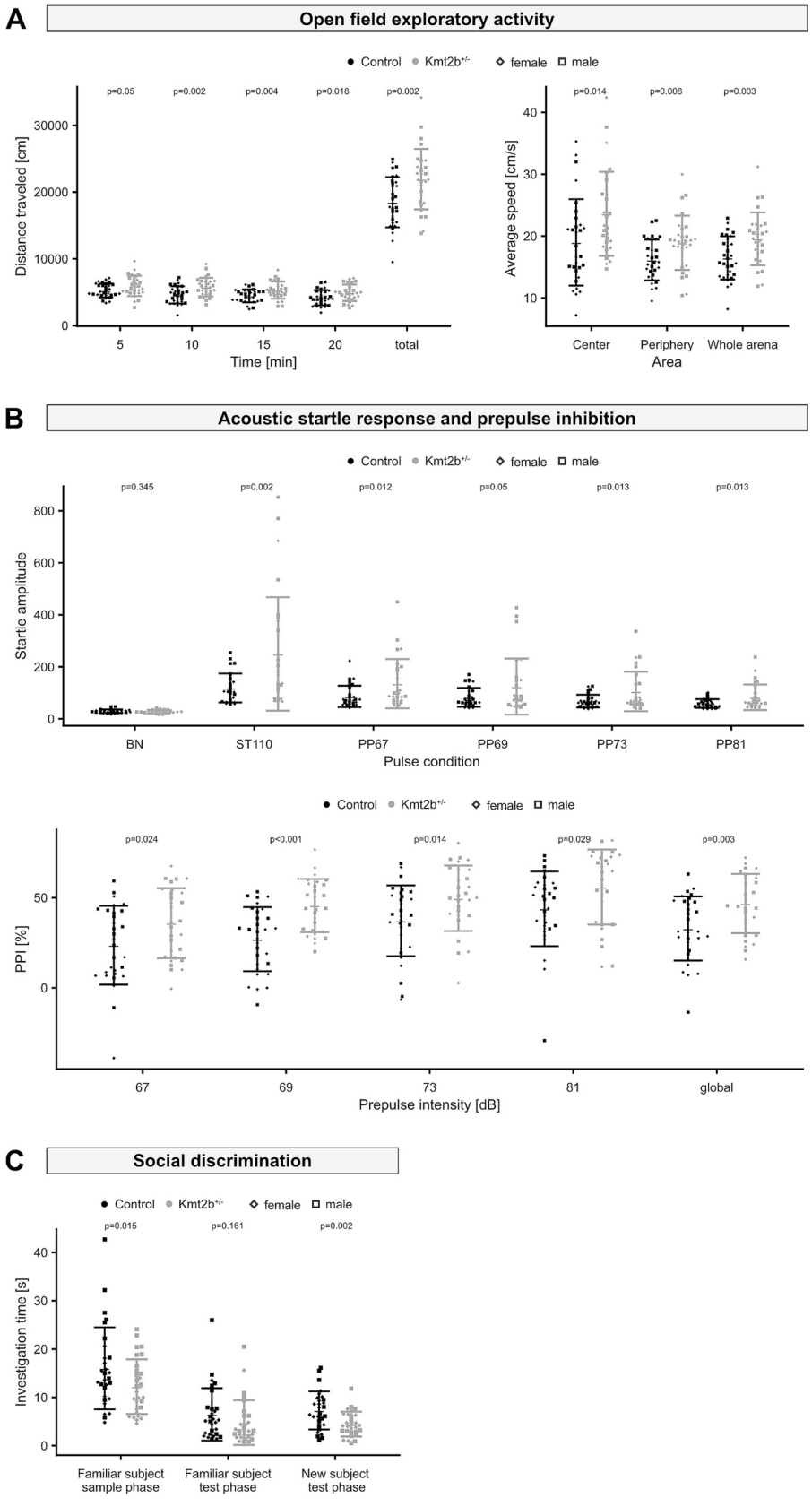

(caption on next page)

Fig. 2. Hyperlocomotion, enhanced acoustic startle and prepulse inhibition, and reduced social investigation in *Kmt2b* knockout mice. (A) Open field test at 9 weeks of age ($N = 29$ *Kmt2b* knockouts, $N = 30$ littermate controls). Left: distance travelled in successive 5-min intervals and across the full 20-min session. Right: average speed in the centre, the periphery and the whole arena. Knockout mice travelled further and moved faster than controls. (B) Acoustic startle response and prepulse inhibition at 9 weeks of age. Top: startle amplitude under background noise alone (BN, 65 dB), under each of the four prepulse conditions (PP67, PP69, PP73, PP81) and in response to the 110 dB startle-alone pulse (ST110). Bottom: percentage prepulse inhibition at each prepulse intensity and averaged across intensities (global). Knockout mice showed both increased startle amplitude and increased prepulse inhibition. (C) Social discrimination test at 18 weeks of age, showing olfactory investigation time directed at the familiar stimulus animal during the sample and test phases and at the novel animal during the test phase. Data are shown as individual animal values with mean ± SD. *p*-values are genotype effects from two-way ANOVA with Tukey post-hoc comparisons and are given above each condition. Complete datasets are provided in Supplementary Tables S1–S3.

significant differences on the rotarod were detected when mice were tested at 11 weeks of age (Supplementary Fig. S1), suggesting that impaired absolute forelimb muscle strength did not generalise to other forelimb-demanding tasks.

The balance beam task revealed clear motor deficits in 29-week-old *Kmt2b* knockout mice of both sexes (Fig. 3A). *Kmt2b* knockout mice of both sexes took significantly longer to traverse the beam than controls at every beam width, and made significantly more stops at all widths except 18 mm in females (Fig. 3A). In *Kmt2b* knockout mice, we observed a consistent 'claw-like' posture of the hindpaws, characterized by abnormal inward flexion of the digits (Fig. 4A). Notably, this aberrant posture was not confined to the slip phase of the task but persisted during the subsequent recovery movements (Fig. 4B). Although partial extension of the digits occasionally occurred, the hindpaws remained predominantly in an abnormally flexed position throughout beam traversal. The posture was present in all three *Kmt2b* knockout animals analysed and in none of the three littermate controls ($p = 0.050$, one-sided Fisher's exact test).

In the ladder rung walking test, 30-week-old female *Kmt2b* knockout mice paused more frequently relative to littermate controls ($p = 0.031$), but this did not – in turn – lead to significantly increased latency to cross (Fig. 3B, Supplementary video S1). Although the data suggested a comparable directionality of effect, no statistically significant differences were detected in male *Kmt2b* knockout mice. Taken together, the beam and ladder assays indicate that *Kmt2b* deficiency leads to deficits in motor coordination and balance.

3.4. No impairment of nociception or genotype-dependent metabolic effects

In the hotplate test of acute thermal pain response, no significant genotype differences were observed in either the latency to first response (hindpaw lick or shake) or second response at 23 weeks of age ($N = 29$ *Kmt2b* knockouts and $N = 29$ littermate controls;

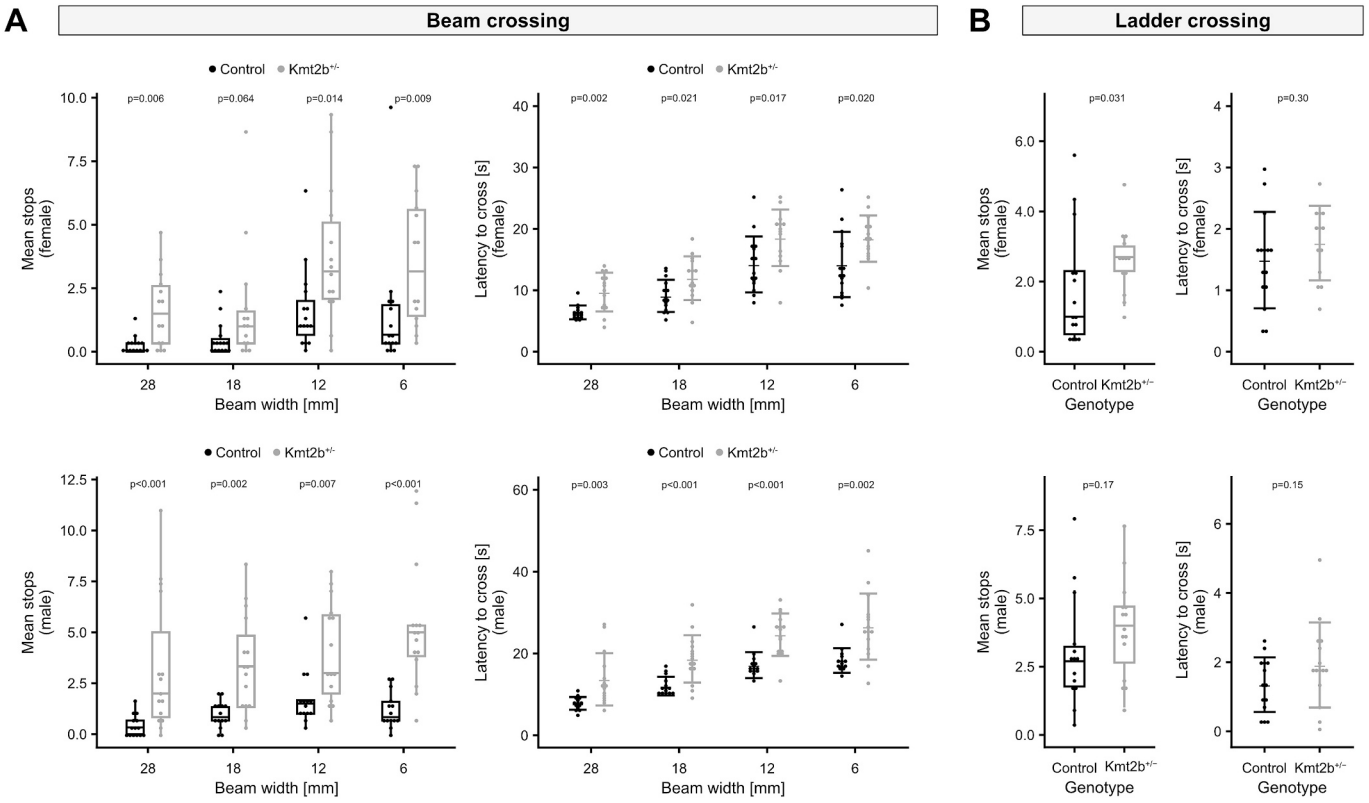

Fig. 3. Impaired motor coordination on the balance beam and horizontal ladder in *Kmt2b* knockout mice. (A) Balance beam test at 29 weeks of age ($N = 29$ *Kmt2b* knockouts, $N = 29$ littermate controls) at four beam widths (28, 18, 12 and 6 mm), shown separately for females (top) and males (bottom). Left: mean number of stops. Right: latency to cross. Knockout mice of both sexes took significantly longer to cross at every beam width and made more stops at all widths except 18 mm in females. (B) Horizontal ladder rung walking test at 30 weeks of age ($N = 28$ *Kmt2b* knockouts, $N = 29$ littermate controls), showing mean number of stops (left) and latency to cross (right) for females (top) and males (bottom). Female knockout mice stopped significantly more frequently than controls without a significant increase in latency to cross; male knockouts showed the same directional trend without reaching significance. Stop counts on both the balance beam and the ladder violated the assumption of normality; these were analysed by Wilcoxon rank-sum (Mann–Whitney U) tests separately by sex and are displayed as box-and-whisker plots showing the median, first and third quartiles, with whiskers extending to a maximum of 1.5× the interquartile range. Latency to cross was analysed by unpaired Student's *t*-tests separately by sex and is shown as individual values with mean ± SD. *p*-values are given above each comparison.

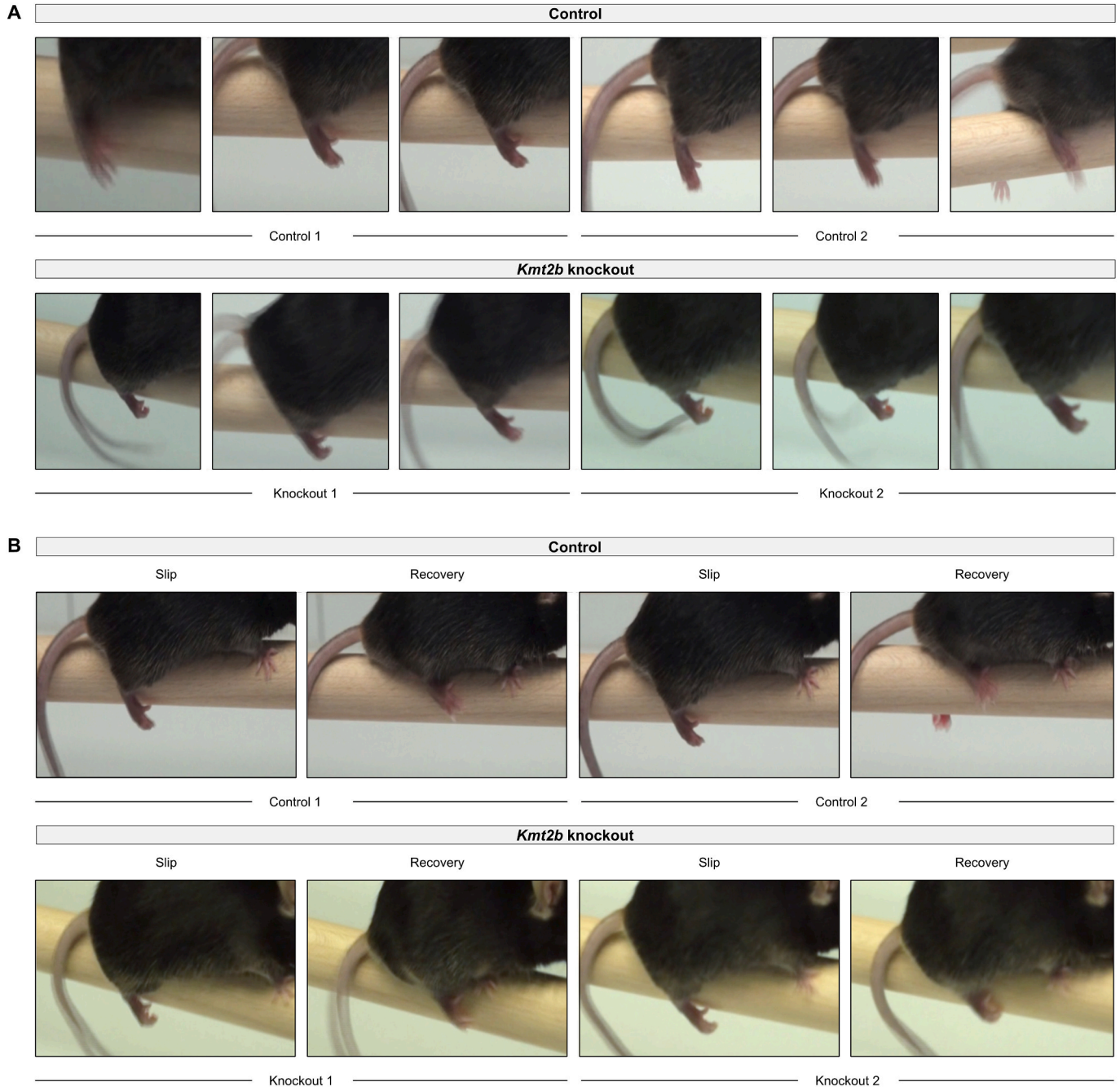

Fig. 4. 'Claw-like' hindpaw posture in *Kmt2b* knockout mice during beam crossing. Frame-by-frame analysis of balance beam video recordings from $N = 3$ male *Kmt2b* knockout mice and $N = 3$ male littermate controls. (A) Consecutive frames from two representative control animals (upper row) and two representative *Kmt2b* knockout animals (lower row) during beam traversal, showing the abnormal inward flexion of the hindpaw digits in knockout mice. (B) Frames captured during a slip and the subsequent recovery for the same animals, showing that the abnormal digit flexion is not confined to the slip itself but persists into post-slip recovery. Although partial extension of the digits occurred intermittently, knockout hindpaws remained predominantly in an abnormally flexed position throughout beam traversal. The posture was present in all three knockout animals analysed and in none of the three controls ($p = 0.050$, one-sided Fisher's exact test); penetrance therefore appeared complete in this sample but requires confirmation in a larger cohort.

Supplementary Tables S5 and S6). Comprehensive clinical chemistry and haematological profiling revealed no significant differences between knockouts and controls besides a small reduction in plasma calcium ($p = 0.009$) and creatinine ($p = 0.022$), both within reference ranges, in heterozygous *Kmt2b* knockout mice (Supplementary Tables S7 and S8), indicating that metabolic and organ functions were largely normal at 39 weeks of age ($N = 28$ *Kmt2b* knockouts and $N = 29$ littermate controls; Supplementary Tables S8-S10). Eye examinations (optokinetic drum for visual acuity) revealed no deficit in visual function in knockouts at 22 weeks of age ($N = 7$ of each sex and genotype; $N = 28$ total; Supplementary Table S11). Overall, *Kmt2b* knockout mice did not show overt abnormalities in other organ systems, pointing to a specific impact of *Kmt2b* deficiency on neurobehaviour.

3.5. Striatal transcriptomic changes in Kmt2b knockout mice

To confirm reduced *Kmt2b* expression and to place the behavioural findings in a molecular context, we performed RNA sequencing on

striatal tissue from *Kmt2b* knockout mice and littermate controls ($N = 12$; $N = 6$ per genotype). *Kmt2b* was the most significantly affected transcript in the dataset, reduced to approximately half of control levels in knockout animals (baseMean of 1183, $\log_2$ fold change −0.98, adjusted $p = 5.8 \times 10^{-42}$; Fig. 5A; Supplementary Table S12). This closely matches a $\log_2$ fold change of −1 expected from loss of one functional allele and confirms *Kmt2b* haploinsufficiency at the transcript level in the target tissue.

Differential expression analysis identified 177 genes with significantly altered striatal expression (adjusted $p < 0.05$), of which 140 were downregulated and 37 upregulated in knockout mice (Fig. 5B; Supplementary Table S12). The predominance of downregulation is consistent with the role of KMT2B as an H3K4 methyltransferase associated with transcriptional activation (Barbagiovanni et al., 2018).

Gene set enrichment analysis against Gene Ontology Biological Process terms identified significantly enriched gene sets falling broadly into three groups (Supplementary Fig. S2), alongside further terms relating to immune response signalling, cytoskeletal organisation and intracellular signal transduction. The first related to neural development and glial biology, including gliogenesis, glial cell differentiation, ensheathment of neurons, neural precursor cell proliferation, cell fate commitment, Wnt signalling, and developmental and anatomical structure maturation. The second related to mitochondrial biology, comprising mitochondrial translation and mitochondrial gene expression. The third comprised terms relating to meiotic chromosome organisation, including synaptonemal complex assembly and organisation. The biological significance of these terms in striatal tissue is unclear, and the transcripts concerned (including *Sycp3*, *Rec8*, *Rnf17*, *Tdrd1* and *Prss50*) were expressed at low absolute levels.

Among the individually significant differentially expressed genes was *Maob*, encoding monoamine oxidase B, which was modestly but significantly downregulated in *Kmt2b* knockout mice (baseMean of 1406, $\log_2$ fold change −0.37, adjusted $p = 3.1 \times 10^{-9}$). *En2*, encoding a homeodomain transcription factor, was among the most strongly upregulated genes (baseMean of 33, $\log_2$ fold change +1.58, adjusted $p = 8.2 \times 10^{-10}$; Supplementary Table S12).

4. Discussion

Our study provides the first comprehensive in vivo behavioural characterization of *Kmt2b* deficiency, revealing a spectrum of neurobehavioural abnormalities. Tests were chosen with focus on unbiased assessment of basic behaviour, motor and sensory domains in order to test for dystonia-related phenotypes but also possible additional phenotypes. Heterozygous *Kmt2b* knockout mice recapitulated several features reminiscent of human KMT2B-related dystonia, including reduced growth (paralleling the short stature seen in several patients (Cif et al., 2020)) and motor coordination deficits, with dystonic-like posturing of the hindpaws during beam crossing (Fig. 4). Our results revealed that one functional *Kmt2b* allele is sufficient for viability and vitality, but insufficient to secure normal motor control and coordination when these features are specifically challenged.

Motor Phenotypes and Subclinical Circuit Dysfunction: Despite the lack of spontaneous dystonic-like signs, *Kmt2b* knockout mice showed clear impairments in skilled motor tasks with signs of dystonic-like paw posturing, which was observed in all three *Kmt2b* knockout animals analysed and in none of the three littermate controls ($p = 0.050$, one-sided Fisher's exact test). Penetrance therefore appeared to be complete in this sample. However, given the small number of animals frame-by-frame analysis was performed on, this remains to be confirmed in a larger cohort.

On the balance beam, *Kmt2b* knockouts of both sexes had an increased latency to cross and hesitated more; on the irregular ladder rung assay, female knockouts hesitated more without a significant increase in latency to cross. Together these indicate deficits in balance, coordination, and/or motor planning. Notably, these tasks were more sensitive in unmasking motor deficits than the accelerating rotarod, on which knockouts did not show significant differences (Supplementary Fig. S1). A similar pattern is reported in other dystonia models: Dyt1 knockdown mice showed no baseline dystonic posturing but manifested impaired beam-walking performance (Dang et al., 2006), confirmed by a recent study of conditional Dyt1 knockouts mice showing age-dependent emergence of beam-walking and rotarod deficits in the

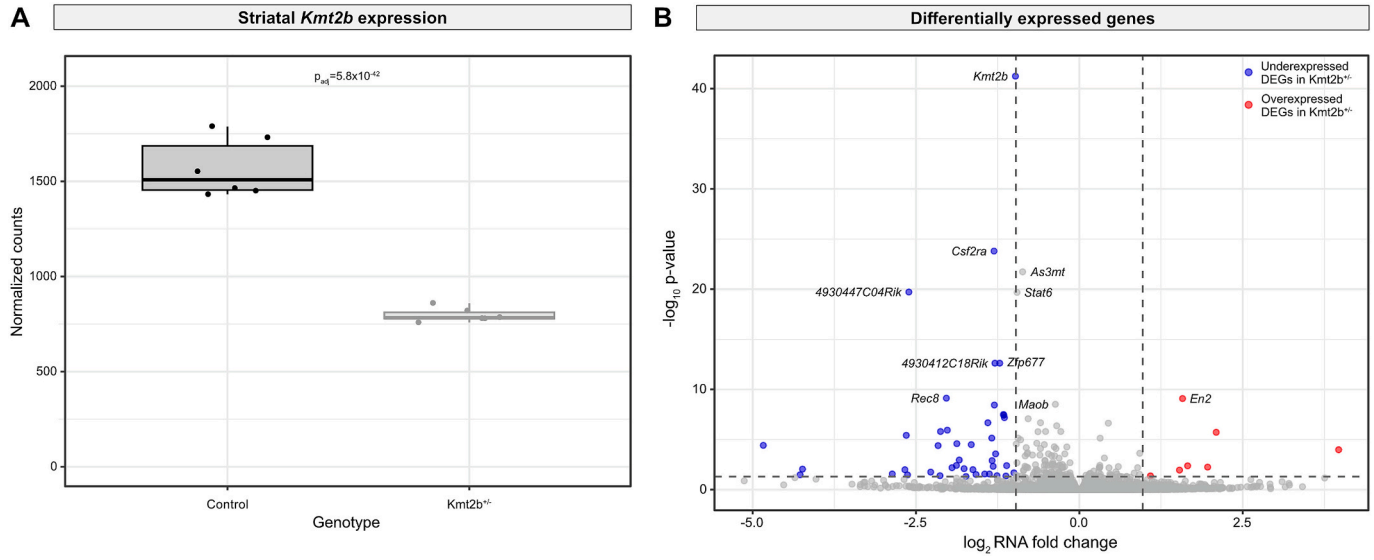

Fig. 5. Striatal transcriptomic changes in *Kmt2b* knockout mice. (A) Normalised *Kmt2b* counts in striatal tissue from *Kmt2b* knockout mice and littermate controls ($N = 6$ per genotype, 39 weeks of age). *Kmt2b* transcript was reduced to approximately half of control levels, consistent with loss of one functional allele ($\log_2$ fold change −0.98, Benjamini-Hochberg adjusted $p = 5.8 \times 10^{-42}$). (B) Volcano plot of differential expression, showing $\log_2$ fold change against $-\log_{10}$ adjusted *p*-value. The horizontal dashed line indicates the significance threshold (adjusted $p = 0.05$) and the vertical dashed lines an absolute $\log_2$ fold change of 1. Genes meeting both criteria are shown in blue (reduced expression in knockout mice) or red (increased expression). The fold-change criterion applies to the colour coding only; the 177 differentially expressed genes reported were defined by adjusted $p < 0.05$ alone. The ten most significantly differentially expressed genes are labelled. *Kmt2b* was the most significantly affected transcript in the dataset. Complete differential expression results are provided in Supplementary Table S12, and gene set enrichment analysis in Supplementary Fig. S2. (For interpretation of the references to colour in this figure legend, the reader is referred to the web version of this article.)

absence of overt dystonic movements (Berryman et al., 2023). Likewise, heterozygous *Gnal* knockout mice (modelling DYT25 dystonia) do not display spontaneous dystonia yet exhibit subtle motor deficits unless challenged pharmacologically (Pelosi et al., 2017; Yu-Taeger et al., 2020). These parallels suggest that *Kmt2b* knockout mice, much like other dystonia mouse models, harbour latent dysfunction in motor circuits that manifests as poor performance during challenging tasks in the absence of spontaneous dystonic-like movements. Consistent with this, we observed that *Kmt2b* knockouts showed grasping difficulties based on paw positioning or slid their hindlimbs on the balance beam (Fig. 4). It is possible that this represents a subclinical dystonia-like feature – an inability to properly coordinate hindlimb movements under balance demands – even though spontaneous dystonic episodes were not seen in typical housing conditions.

The absence of spontaneous dystonic posturing in *Kmt2b* knockout mice is consistent with a well-recognized pattern in genetic dystonia models and does not imply an intrinsic inability of the murine nervous system to generate dystonic movements, which can be provoked by targeted pharmacological perturbation of cerebellar circuits in otherwise neurologically intact rodents (van der Heijden and Sillitoe, 2023). Several mechanisms likely contribute to the attenuated phenotype observed in constitutive germline models. Early developmental disruption of gene function may allow compensatory neural reorganization - a concept supported experimentally in DYT1 models, where acute cerebellar knockdown of torsinA in adult mice produces severe dystonia whereas equivalent knockdown during early postnatal development does not (Fremont et al., 2017). Importantly, a reduction of at least ~60% in torsinA protein was required to elicit overt dystonia (Fremont et al., 2017). Our transcriptomic data place the present model in this context: heterozygous loss reduced striatal *Kmt2b* transcript by approximately half (Fig. 5A), a reduction below the threshold that was required to elicit overt dystonia in the torsinA model. A comparable dose dependence for KMT2B has not been established, but this offers a parsimonious account of why one functional allele is compatible with normal appearance and vitality while producing deficits that emerge only under specific task demands.

A further consideration concerns the genetic background of the model itself. Genetic background and modifier effects modulate phenotypic expressivity in dystonia mouse models (Tanabe et al., 2012). Mice were backcrossed onto C57BL/6JolaHsd for at least four generations, which reduces the expected contribution of the E14 embryonic stem cell donor genome from 50% to approximately 3%, rather than to the ~0.05% achieved by the ten generations conventionally required for a fully congenic line. Residual donor-derived genomic segments, particularly those linked to the targeted locus, could therefore contribute to the phenotypes reported here. Four generations is the minimum accepted for phenotyping at the German Mouse Clinic and represents a deliberate compromise between residual background contribution and the additional time and animal numbers required for further backcrossing, in keeping with 3R principles. Because all comparisons were made against wild-type littermates from heterozygous intercrosses, background effects unlinked to the targeted allele are expected to be distributed evenly between genotypes.

Finally, standard laboratory conditions may not reproduce the physiological and environmental stressors that can act as 'second hits' to precipitate overt motor symptoms in genetically predisposed individuals – a mechanism increasingly recognized in human dystonia research (Rauschenberger et al., 2021). Together, these factors likely explain why motor coordination deficits and dystonic-like paw posturing in *Kmt2b* knockout mice manifest only under specific task demands and support the use of pharmacological or environmental challenges in future studies to unmask the full phenotypic spectrum. Consistent with this, the single isolated tremor-like episode observed during handling in one *Kmt2b* knockout female may represent a low-penetrance stress-sensitive paroxysmal event of the kind predicted by the second-hit hypothesis (Rauschenberger et al., 2021), warranting systematic investigation under defined stressors in future work combined with detailed time course analyses.

Phenotype across the testing window: Each behavioural domain was assessed once, at a single age, so the present design cannot separate age effects from differences in assay sensitivity. Body weight was the only parameter measured repeatedly and is therefore the only one permitting a direct statement about time. Knockout mice of both sexes weighed significantly less than controls from the first assessment at 9 weeks; in females this difference remained significant at every subsequent timepoint through 39 weeks ($p = 0.045$), whereas in males it ceased to reach significance from 29 weeks onward (Fig. 1A). We do not interpret the latter as resolution of the growth phenotype: the difference persisted in females assessed at identical ages, and body length at 39 weeks was significantly reduced in both sexes (females $p = 0.008$, males $p = 0.001$). The growth deficit is therefore established by 9 weeks and still demonstrable at 39, with no indication of progressive worsening. Body weight cannot, however, substitute for the motor, sensorimotor or social domains, each assessed at a single age; whether those phenotypes are stable, progressive or emergent is not addressed by the present design and is the focus of prospective longitudinal work.

Hyperlocomotion and Sensorimotor Gating: Knockouts of both sexes were significantly more mobile in the open field test than wild-type littermates, covering greater distances at higher speeds. The absence of genotype-dependent differences in centre exploration suggests that this phenotype is unlikely to reflect altered anxiety-related behaviour, but rather increased baseline locomotor activity or altered behavioural responses to novel environments. Hyperdopaminergic states or frontostriatal circuit disinhibition are known to produce hyperlocomotion in rodents (Zhuang et al., 2001), raising the question of whether KMT2B deficiency may lead to dysregulated neuronal circuit activity. In line with this, prior work on DYT1 models found that torsinA deficiency causes increased exploratory activity and motor hyperactivity (Dang et al., 2006), potentially related to altered striatal dopamine signalling (Yokoi et al., 2011). Future neurochemical studies of *Kmt2b* knockout mice - measuring striatal dopamine and trace-amine levels, turnover, and receptor binding - could clarify whether a similar mechanism underlies their hyperactive behaviour.

In addition to hyperlocomotion, *Kmt2b* knockout mice exhibited an exaggerated acoustic startle response and increased PPI. Elevated PPI indicates unusually strong sensorimotor gating, the neural process that filters out extraneous stimuli (Gómez-Nieto et al., 2020). This is an unexpected finding, as some neuropsychiatric and basal ganglia disorders (including the blink reflex in cervical dystonia (Öztürk et al., 2016)) have been associated with reduced PPI or altered gating. One possible interpretation is that *Kmt2b* deficiency might lead to alterations in synaptic plasticity or overactivity of inhibitory interneuron circuits in the brainstem and/or basal ganglia that mediate PPI. Alternatively, the enhanced PPI could be a consequence of the knockouts' heightened startle reactivity – since their baseline startle is higher, the relative dampening by a prepulse appears greater. Regardless, the abnormal PPI points to altered sensorimotor integration in *Kmt2b* knockouts. Notably, abnormalities in temporal discrimination and sensory processing are recognized in many basal ganglia diseases including adult-onset dystonia (Conte et al., 2017). It is conceivable that *KMT2B* deficiency alters the developmental tuning of these circuits. Further studies measuring neurotransmitter activity could shed light on the neural mechanisms underlying the combination of hyperactivity, heightened startle, and increased PPI observed in *Kmt2b* knockout mice.

The combination of enhanced acoustic startle reactivity, enhanced prepulse inhibition and hyperlocomotion is consistent with altered dopaminergic modulation of sensorimotor and corticostriatal circuits, although the direction of the gating change is opposite to that reported in several basal ganglia disorders. Increased startle and hyperlocomotion are compatible with a shared circuit-level mechanism. The reduced body weight is plausibly secondary to increased locomotor activity and is not by itself diagnostic of that interpretation. A comparable

combination has been reported in rats, where selective chemogenetic activation of nigrostriatal dopamine neurons increased locomotion and, in females, prepulse inhibition (Casado-Sainz et al., 2022). The correspondence is limited - acute activation in a different species, with a sex-specific gating effect - but it shows that increased striatal dopaminergic tone can raise, rather than lower, prepulse inhibition.

Our transcriptomic data identify a candidate entry point. *Maob*, encoding monoamine oxidase B, was significantly reduced in striatum of *Kmt2b* knockout mice ($\log_2$ fold change −0.37, adjusted $p = 3.1 \times 10^{-9}$; Supplementary Table S12). The likely functional consequence is not a simple increase in dopaminergic tone. Although both monoamine oxidase isoenzymes oxidise dopamine in vitro, MAO-A rather than MAO-B is the principal route of dopamine catabolism in rodent brain. Mice lacking MAO-B show a marked increase in β-phenylethylamine with essentially unchanged brain dopamine and serotonin (Grimsby et al., 1997), and striatal microdialysis in these animals shows no alteration of dopamine metabolism (Fornai et al., 1999). Reduced MAO-B activity would therefore be expected to act principally through trace-amine signalling rather than through dopamine availability.

The observation is nonetheless of interest here, because MAO-B-deficient mice show a behavioural profile that overlaps the one described in this study: heightened responsiveness to novelty and behavioural disinhibition (Bortolato et al., 2009), and impaired within-session habituation of locomotor activity in a novel open field (Lee et al., 2004). Our knockouts likewise travelled further and moved faster in a novel arena, with no genotype difference in the proportion of time or distance spent in the centre (Supplementary Table S1). The correspondence is only partial: MAO-B-deficient mice additionally show reduced anxiety-like behaviour, which we did not observe, and we have not measured MAO-B protein or enzyme activity. A second, non-exclusive possibility is that the *Maob* change forms part of the glial signature identified by gene set enrichment analysis, since MAO-B in brain is expressed predominantly by astrocytes. Should dopaminergic tone prove to be altered in this model, the direction of any consequent effect on sensorimotor gating could not be predicted from dopamine availability alone, being receptor-subtype- and region-specific and dependent on baseline gating (Roussos et al., 2008; Giakoumaki et al., 2007).

This remains hypothesis-generating. The *Maob* expression change is modest and was measured at transcript level only. No gene encoding a component of dopamine synthesis, transport, vesicular packaging or receptor signalling, nor the alternative catabolic enzymes Maoa and Comt, reached significance in our dataset. Direct measurement of striatal monoamine and trace-amine content and turnover, together with MAO-B protein and enzyme activity, will be required before this observation can be interpreted mechanistically.

Social and Cognitive Behaviours: *Kmt2b* knockout mice displayed reduced social investigatory behaviour, spending significantly less time in olfactory investigation of an unfamiliar conspecific than littermate controls, suggesting a reduced drive to engage in novel social interactions. This reduction in social investigation is consistent with the autism spectrum disorder features reported in a subset of KMT2B mutation carriers – autism spectrum disorder has been documented in 14.3%, and psychiatric features including attention deficit hyperactivity disorder and anxiety in 42.9% of patients in a KMT2B cohort (Cif et al., 2020) - though general hypomotivation in an unfamiliar context cannot be excluded as an alternative explanation. The normal performance of *Kmt2b* knockouts on the social recognition index indicates that social memory ability is largely intact, suggesting the deficit reflects reduced social motivation rather than an impairment of social cognition per se. Reduced olfactory investigation was unlikely to reflect hyperlocomotion alone, as the recognition index - a within-subject measure normalised to total investigation time - did not differ between genotypes, indicating that knockouts retained a normal relative preference for the novel over the familiar stimulus despite their reduced overall investigation time.

Consistent with this broader pattern of altered social behaviour, *Kmt2b* knockout mice also showed reduced vocalisation in response to gentle handling in the SHIRPA screen (Supplementary Table S4). The reduced vocalisation in response to gentle handling is difficult to interpret in isolation – it could reflect reduced nociceptive sensitivity, altered autonomic reactivity, or diminished social signalling - any of which would be consistent with the broader neurobehavioural profile of *Kmt2b* knockout mice, though the hotplate test did not reveal differences in acute thermal pain sensitivity (Supplementary Tables S5 and S6). On the other hand, it might be related to an altered behavioural response to novel environments seen in the OF test.

Transcriptomic signatures of *Kmt2b* haploinsufficiency: Gene set enrichment analysis indicated a coordinated shift in gene sets related to neural development and glial biology, including gliogenesis, glial cell differentiation, ensheathment of neurons, neural precursor cell proliferation, cell fate commitment and Wnt signalling. This signal derives from the distribution of these gene sets across the ranked transcriptome rather than from a small number of large individual effects: no canonical astrocytic, oligodendrocytic or gliogenic transcript reached the adjusted significance threshold in our dataset (Supplementary Fig. S2, Supplementary Table S12). The pattern is therefore one of many small, concordant changes, which is what would be expected from partial loss of a broadly acting chromatin regulator, but it is correspondingly less robust than a gene-level result and requires orthogonal confirmation.

The shift is consistent with the known molecular function of KMT2B, which acts preferentially at bivalent promoters to maintain the poised chromatin state of developmentally regulated genes (Glaser et al., 2009; Denissov et al., 2014), and indicates that developmental transcriptional programmes remain measurably altered in adult striatum. An alternative reading has to be considered, since enrichment of gliogenesis and glial differentiation terms in adult tissue is also compatible with reactive gliosis. Gene sets relating to immune response signalling were likewise among the enriched terms (Supplementary Fig. S2); enrichment, however, reflects the distribution of set members across the ranked transcriptome and does not by itself indicate the direction of change. The available evidence argues against a substantial reactive response. Among canonical markers of astrocytic and microglial reactivity, only *Serpina3n* reached the adjusted significance threshold, and modestly so ($\log_2$ fold change +0.31, adjusted $p = 0.006$); *Gfap, Vim, Lcn2, C3, Cd68, Aif1, Trem2* and *Cx3cr1* were not among the significantly differentially expressed genes (Supplementary Table S12), and immune-signalling genes that did reach significance - *Csf2ra, Stat6* and *Stat4* - were all downregulated. We, however, did not formally test for a reactive glial response, and sub-threshold changes cannot be excluded.

Gene sets relating to mitochondrial translation and mitochondrial gene expression were also among those significantly enriched. H3K4 methylation has been shown to regulate the expression of genes governing mitochondrial function. Reduction of global H3K4 methylation in mouse oocytes alters expression of mitochondrial regulators and is accompanied by mitochondrial abnormalities (Mei et al., 2023), indicating that mitochondrial gene programmes are among the transcriptional outputs sensitive to this chromatin mark.

Defects in nuclear-encoded mitochondrial disease genes account for approximately 13% of genetically resolved dystonia diagnoses (Indelicato et al., 2024), so mitochondrial biology is an established contributor to dystonia pathophysiology. We stress that these data establish only that these gene sets are coordinately shifted within the ranked transcriptome. No functional assessment of mitochondrial activity was performed, and few mitochondrial transcripts were individually differentially expressed. This observation therefore identifies a direction for future work rather than evidence of mitochondrial impairment.

Comparison with the IMPC broad-spectrum phenotyping dataset: A heterozygous *Kmt2b* knockout line has also been characterized by the International Mouse Phenotyping Consortium (IMPC) within their standardised phenotyping pipeline (Dickinson et al., 2016; Groza et al., 2023), with gene-specific data publicly available via the IMPC portal (https://www.mousephenotype.org/data/genes/MGI:109565). At the

IMPC discovery threshold of $p < 1 \times 10^{-4}$, significant effects were reported for integument, pigmentation, hematopoietic, and homeostasis/metabolism domains, but not for any of the behavioural domains assessed for this line within the IMPC pipeline; balance beam, ladder rung walking, and rotarod were not assessed. The apparent discrepancy with our neurobehavioural findings is largely explicable by methodological differences: the IMPC analyses small fixed cohorts (7 males and 7 females per line) against centre- and sex-specific historical controls with a stringent threshold appropriate for genome-wide screening, whereas we used sex-matched littermate controls, 15 animals per sex and genotype, a neurodevelopment-focused pipeline chosen a priori, and parameter-specific statistical approaches. Allelic and substrain differences may further contribute to phenotypic divergence. Our study therefore illustrates that broad-spectrum screens and hypothesis-led, disease-focused phenotyping are genuinely complementary: assays such as balance beam, ladder rung walking, and frame-by-frame video analysis of paw posture - selected a priori based on the clinical features of KMT2B-related dystonia - were able to resolve motor-coordination and dystonic-like phenotypes that were not captured by the standardised IMPC pipeline. This supports a broader case for pairing systematic phenotyping resources with targeted, disease-relevant deep phenotyping.

This study provides, to our knowledge, the first systematic behavioural characterization of a *Kmt2b* haploinsufficient mouse, and its primary contribution is the demonstration that a single functional *Kmt2b* allele is sufficient for viability but not for normal motor, sensorimotor, and social function across several convergent domains. This behavioural foundation was a necessary prerequisite: without first establishing which circuits are functionally affected and to what degree, subsequent molecular and histopathological work would lack clear targets and risk being poorly directed. At the same time, we recognise that a purely behavioural dataset cannot on its own establish causal molecular mechanisms, and the present manuscript is correspondingly limited in this respect. Comprehensive histopathological characterization of relevant brain regions, confirmation of reduced *Kmt2b* expression at the protein level, and direct neurochemical measurement of striatal dopamine turnover and related signalling pathways all remain to be established. We were able to draw on RNA-seq data from this cohort to provide one piece of molecular support, in the form of significantly reduced *Maob* expression, which identifies monoamine oxidase B and trace-amine signalling as a specific candidate pathway linking *Kmt2b* haploinsufficiency to the locomotor phenotype; however, this single transcriptomic observation should be regarded as a starting point rather than a substitute for broader mechanistic validation. Systematic transcriptomic and proteomic profiling across brain regions, together with longitudinal time course analyses spanning early to mature adulthood, are the focus of ongoing follow up work and will be needed to translate the phenotypic findings reported here into a mechanistic understanding of *KMT2B*-related dystonia.

Implications for Dystonia and Human Disease: In summary, although *Kmt2b* knockout mice do not manifest the overt generalized dystonia as seen in patients, the constellation of phenotypes we observe – hyperlocomotion, altered sensorimotor gating, impaired fine motor coordination with signs of dystonic-like paw posturing, and reduced social interaction – paints a picture of a widespread neurological impact. This is consistent with the complex clinical presentation of *KMT2B* mutation carriers, who often have mixed motor, cognitive, and psychiatric features that vary in penetrance and expressivity (Cif et al., 2020).

Future integration of behavioural phenotyping with molecular and physiological analyses in this model will help to elucidate how KMT2B deficiency contributes to motor circuit dysfunction and may inform the development of mechanism-based treatments for KMT2B-related dystonia.

Supplementary data to this article can be found online at https://doi.org/10.1016/j.nbd.2026.107608.

CRediT authorship contribution statement

Philip Harrer: Writing – original draft, Visualization, Project administration, Formal analysis, Conceptualization. **Andrea Kranz:** Writing – review & editing, Resources, Methodology, Investigation. **Lore Becker:** Writing – review & editing, Methodology, Investigation, Formal analysis. **Lillian Garrett:** Writing – review & editing, Methodology, Investigation, Formal analysis. **Sabine M. Hölter:** Writing – review & editing, Methodology, Investigation, Formal analysis. **Adrián Sanz-Moreno:** Writing – review & editing, Methodology, Investigation, Formal analysis. **Oana V. Amarie:** Writing – review & editing, Methodology, Investigation, Formal analysis. **Birgit Rathkolb:** Writing – review & editing, Resources, Methodology, Investigation, Formal analysis. **Stefanie Leuchtenberger:** Writing – review & editing, Methodology, Investigation, Formal analysis. **Valerie Gailus-Durner:** Writing – review & editing, Supervision, Resources, Project administration. **Helmut Fuchs:** Writing – review & editing, Supervision, Resources, Project administration. **Martin Hrabě de Angelis:** Writing – review & editing, Supervision, Resources, Funding acquisition. **Alice Saparov:** Writing – review & editing, Methodology, Investigation, Formal analysis. **Celestine Sieber:** Writing – review & editing. **Volker Kittke:** Writing – review & editing. **Nazanin Mirza-Schreiber:** Writing – review & editing. **A. Francis Stewart:** Writing – review & editing, Supervision, Resources, Methodology. **Juliane Winkelmann:** Writing – review & editing, Supervision, Resources, Funding acquisition. **Konrad Oexle:** Writing – review & editing, Supervision. **Amanda Pocratsky:** Writing – review & editing, Methodology, Investigation, Formal analysis. **Michael Zech:** Writing – review & editing, Supervision, Funding acquisition, Conceptualization.

Declaration of generative AI and AI-assisted technologies in the writing process

During the preparation of this work, the authors used Grammarly to improve language and readability. After using this tool, the authors reviewed and edited the content as needed and take full responsibility for the content of the publication.

Funding

This work was supported by a “Schlüsselprojekt” grant from the Else Kröner-Fresenius-Stiftung (2022_EKSE.185). This research was also supported by funding from the EJP RD (EJP RD Joint Transnational Call 2022) and the German Federal Ministry of Education and Research (BMBF, Bonn, Germany), awarded to the project PreDYT (PREdictive biomarkers in DYsTonia, 01GM2302) and the Infrafrontier grant 01KX1012 (MHdA). In addition, this study (M.Z.) has received funding from the Federal Ministry of Education and Research (BMBF) and the Free State of Bavaria under the Excellence Strategy of the Federal Government and the Länder, as well as by the Technical University of Munich - Institute for Advanced Study and the German Center for Diabetes Research (DZD) (MHdA).

Declaration of competing interest

The authors declare that they have no known competing financial interests or personal relationships that could have appeared to influence the work reported in this paper.

Acknowledgement

We thank the GMC technicians' team for expert technical help and acknowledge the technical support of Core Facility Laboratory Animal Services at Helmholtz Munich.

Data availability

Raw and processed RNA sequencing data generated in this study have been deposited in the NCBI Gene Expression Omnibus (GEO: GSE346547). All other data supporting the findings of this study are available from the corresponding author upon reasonable request.

References

Barbagiovanni, G., et al., 2018. KMT2B is selectively required for neuronal transdifferentiation, and its loss exposes dystonia candidate genes. Cell Rep. 25 (4), 988–1001.

Berryman, D., et al., 2023. Motor deficit and lack of overt dystonia in dlx conditional Dyt1 knockout mice. Behav. Brain Res. 439, 114221.

Bortolato, M., et al., 2009. Behavioral disinhibition and reduced anxiety-like behaviors in monoamine oxidase B-deficient mice. Neuropsychopharmacology 34 (13), 2746–2757.

Carecchio, M., et al., 2019. Frequency and phenotypic spectrum of KMT2B dystonia in childhood: a single-center cohort study. Mov. Disord. 34 (10), 1516–1527.

Casado-Sainz, A., et al., 2022. Dorsal striatal dopamine induces fronto-cortical hypoactivity and attenuates anxiety and compulsive behaviors in rats. Neuropsychopharmacology 47 (2), 454–464.

Cif, L., et al., 2020. KMT2B-related disorders: expansion of the phenotypic spectrum and long-term efficacy of deep brain stimulation. Brain 143 (11), 3242–3261.

Ciolfi, A., et al., 2021. Childhood-onset dystonia-causing KMT2B variants result in a distinctive genomic hypermethylation profile. Clin. Epigenetics 13 (1), 157.

Conte, A., et al., 2017. Temporal discrimination: mechanisms and relevance to adult-onset dystonia. Front. Neurol. 8, 625.

Dang, M.T., et al., 2006. Motor deficits and hyperactivity in Dyt1 knockdown mice. Neurosci. Res. 56 (4), 470–474.

Denissov, S., et al., 2014. Mll2 is required for H3K4 trimethylation on bivalent promoters in embryonic stem cells, whereas Mll1 is redundant. Development 141 (3), 526–537.

Dickinson, M.E., et al., 2016. High-throughput discovery of novel developmental phenotypes. Nature 537 (7621), 508–514.

Dobin, A., et al., 2013. STAR: ultrafast universal RNA-seq aligner. Bioinformatics 29 (1), 15–21.

Faundes, V., et al., 2018. Histone lysine methylases and demethylases in the landscape of human developmental disorders. Am. J. Hum. Genet. 102 (1), 175–187.

Fornai, F., et al., 1999. Striatal dopamine metabolism in monoamine oxidase B-deficient mice: a brain dialysis study. J. Neurochem. 73 (6), 2434–2440.

Fremont, R., et al., 2017. A role for cerebellum in the hereditary dystonia DYT1. Elife 6.

Fuchs, H., et al., 2011. Mouse phenotyping. Methods 53 (2), 120–135.

Fuchs, H., et al., 2018. Understanding gene functions and disease mechanisms: phenotyping pipelines in the German mouse clinic. Behav. Brain Res. 352, 187–196.

Garrett, L., et al., 2012. Voluntary wheel running in mice increases the rate of neurogenesis without affecting anxiety-related behaviour in single tests. BMC Neurosci. 13, 61.

Giakoumaki, S.G., et al., 2007. Disruption of prepulse inhibition of the startle reflex by the preferential D(3) agonist ropinirole in healthy males. Psychopharmacology 194 (3), 289–295.

Glaser, S., et al., 2006. Multiple epigenetic maintenance factors implicated by the loss of Mll2 in mouse development. Development 133 (8), 1423–1432.

Glaser, S., et al., 2009. The histone 3 lysine 4 methyltransferase, Mll2, is only required briefly in development and spermatogenesis. Epigenetics Chromatin 2 (1), 5.

Gómez-Nieto, R., Hormigo, S., López, D.E., 2020. Prepulse inhibition of the auditory startle reflex assessment as a Hallmark of brainstem sensorimotor gating mechanisms. Brain Sci. 10 (9).

Grimsby, J., et al., 1997. Increased stress response and beta-phenylethylamine in MAOB-deficient mice. Nat. Genet. 17 (2), 206–210.

Groza, T., et al., 2023. The international mouse phenotyping consortium: comprehensive knockout phenotyping underpinning the study of human disease. Nucleic Acids Res. 51 (D1), D1038–D1045.

Hölter, S.M., et al., 2015a. Tests for anxiety-related behavior in mice. Curr Protoc Mouse Biol 5 (4), 291–309.

Hölter, S.M., et al., 2015b. Assessing cognition in mice. Curr Protoc Mouse Biol 5 (4), 331–358.

Indelicato, E., et al., 2024. Dystonia and mitochondrial disease: the movement disorder connection revisited in 900 genetically diagnosed patients. J. Neurol. 271 (7), 4685–4692.

Kerimoglu, C., et al., 2013. Histone-methyltransferase MLL2 (KMT2B) is required for memory formation in mice. J. Neurosci. 33 (8), 3452–3464.

Kerimoglu, C., et al., 2017. KMT2A and KMT2B mediate memory function by affecting distinct genomic regions. Cell Rep. 20 (3), 538–548.

Lee, M., et al., 2004. MAO-B knockout mice exhibit deficient habituation of locomotor activity but normal nicotine intake. Genes Brain Behav. 3 (4), 216–227.

Love, M.I., Huber, W., Anders, S., 2014. Moderated estimation of fold change and dispersion for RNA-seq data with DESeq2. Genome Biol. 15 (12), 550.

Mei, N.H., et al., 2023. H3K4 methylation promotes expression of mitochondrial dynamics regulators to ensure oocyte quality in mice. Adv Sci 10 (12), e2204794.

Meyer, E., et al., 2017. Mutations in the histone methyltransferase gene KMT2B cause complex early-onset dystonia. Nat. Genet. 49 (2), 223–237.

Mirza-Schreiber, N., et al., 2022. Blood DNA methylation provides an accurate biomarker of KMT2B-related dystonia and predicts onset. Brain 145 (2), 644–654.

Öztürk, O., Gündüz, A., Kızıltan, M.E., 2016. Deficient median nerve prepulse inhibition of the blink reflex in cervical dystonia. Clin. Neurophysiol. 127 (12), 3524–3528.

Pelosi, A., et al., 2017. Heterozygous Gnal mice are a novel animal model with which to study dystonia pathophysiology. J. Neurosci. 37 (26), 6253–6267.

Prusky, G.T., et al., 2004. Rapid quantification of adult and developing mouse spatial vision using a virtual optomotor system. Invest. Ophthalmol. Vis. Sci. 45 (12), 4611–4616.

R Core Team, 2015. R: A Language and Environment for Statistical Computing. R Core Team, Vienna, Austria.

Rauschenberger, L., et al., 2021. Second hit hypothesis in dystonia: dysfunctional cross talk between neuroplasticity and environment? Neurobiol. Dis. 159, 105511.

Rogers, D.C., et al., 1997. Behavioral and functional analysis of mouse phenotype: SHIRPA, a proposed protocol for comprehensive phenotype assessment. Mamm. Genome 8 (10), 711–713.

Roussos, P., Giakoumaki, S.G., Bitsios, P., 2008. The dopamine D(3) receptor Ser9Gly polymorphism modulates prepulse inhibition of the acoustic startle reflex. Biol. Psychiatry 64 (3), 235–240.

Stehr, A.M., et al., 2025. Variable expressivity of KMT2B variants at codon 2565 in patients with dystonia and developmental disorders. Parkinsonism Relat. Disord. 133, 107319.

Tanabe, L.M., Martin, C., Dauer, W.T., 2012. Genetic background modulates the phenotype of a mouse model of DYT1 dystonia. PloS One 7 (2), e32245.

van der Heijden, M.E., Sillitoe, R.V., 2023. Cerebellar dysfunction in rodent models with dystonia, tremor, and ataxia. Dystonia 2.

Wu, T., et al., 2021. clusterProfiler 4.0: a universal enrichment tool for interpreting omics data. Innovation 2 (3), 100141.

Yokoi, F., et al., 2011. Motor deficits and decreased striatal dopamine receptor 2 binding activity in the striatum-specific Dyt1 conditional knockout mice. PloS One 6 (9), e24539.

Yu-Taeger, L., et al., 2020. Impaired dopamine- and adenosine-mediated signaling and plasticity in a novel rodent model for DYT25 dystonia. Neurobiol. Dis. 134, 104634.

Zech, M., et al., 2016. Haploinsufficiency of KMT2B, encoding the lysine-specific histone methyltransferase 2B, results in early-onset generalized dystonia. Am. J. Hum. Genet. 99 (6), 1377–1387.

Zech, M., et al., 2017. KMT2B rare missense variants in generalized dystonia. Mov. Disord. 32 (7), 1087–1091.

Zech, M., Lam, D.D., Winkelmann, J., 2019. Update on KMT2B-related dystonia. Curr. Neurol. Neurosci. Rep. 19 (11), 92.

Zhuang, X., et al., 2001. Hyperactivity and impaired response habituation in hyperdopaminergic mice. Proc. Natl. Acad. Sci. U. S. A. 98 (4), 1982–1987.